



ELSEVIER

Contents lists available at ScienceDirect

# Nuclear Instruments and Methods in Physics Research A

journal homepage: [www.elsevier.com/locate/nima](http://www.elsevier.com/locate/nima)

## Topical Review

# Comparison of theoretical and experimental Cu and Mo K-edge XAS

J.J. Kas<sup>a</sup>, J.J. Rehr<sup>a,\*</sup>, J.L. Glover<sup>b</sup>, C.T. Chantler<sup>b</sup><sup>a</sup> Department of Physics, University of Washington Seattle, WA 98195, USA<sup>b</sup> Department of Physics, University of Melbourne, Melbourne, Vic, Australia

## ARTICLE INFO

Available online 18 January 2010

### Keywords:

X-ray absorption spectra

EXAFS

XANES

Multiple scattering theory

## ABSTRACT

We compare *ab initio* broad spectrum calculations of the K-edge X-ray absorption spectra of copper and molybdenum against accurate experimental measurements and tabulated standards on an absolute scale. Comparisons are also presented for the fine structure in the spectra.

© 2010 Elsevier B.V. All rights reserved.

## 1. Introduction

Accurate theoretical calculations of X-ray absorption spectra (XAS) are essential for quantitative interpretations of the spectra. While theoretical calculations of phase shifts and scattering amplitudes are widely used as standards for extended X-ray absorption fine structure (EXAFS) investigations [1], less attention has been devoted to XAS on an absolute scale over a broad energy range. Recently, however, there has been considerable interest in quantitative measurements of XAS [2]. Moreover there have been a number of theoretical developments [3–8] that call for a careful comparison with experiment. These developments include improved treatments of many-body effects which are implemented in the FEFF9.0 real-space multiple-scattering (RSMS) code [6], such as inelastic losses, core-hole effects, vibrational amplitudes, and the extension to full spectrum calculations of optical constants including solid state effects. There have also been improvements in the theory of the near-edge structure in XAS [7,8]. In view of these advances it is now useful to reassess the quality of modern calculations by comparing with absolute measurements [9–11] and tabulated atomic calculations [12,13].

In this work, we have used the *ab initio* XAS codes FEFF8.4 and FEFF9.0 to calculate both the K-edge EXAFS and XANES spectra of fcc Cu and bcc Mo, as well as the extended spectra over a broad range. The calculations are compared against absolute measurements of mass absorption and standard tabulations based on atomic codes [12,13]. In addition, a comparison of EXAFS fits was performed using the ATHENA and ARTEMIS EXAFS analysis codes [14].

## 2. Comparison of XAS in absolute units

A comparison of theory and high precision experiment in absolute units can provide a sensitive test of various assumptions in the theory. The FEFF9.0 calculations are based on Dirac-Fock calculations of the initial core-states together with a GW quasi-particle treatment of final, continuum states in the presence of a screened core-hole, where  $G$  is the photoelectron Green's function and  $W = \epsilon^{-1} v_{\text{Coulomb}}$  is the screened coulomb interaction. At large energies, i.e., above a crossover energy  $E_x$  where Debye-Waller factors damp out the fine structure, solid state effects in the spectra are neglected. Detailed high-accuracy measurements of the mass absorption coefficient  $\mu(E)/\rho$  of molybdenum [15] are presented in Fig. 1a. The scattering contributions were subtracted from the experimental data before comparison. This experimental data set had absolute point accuracies well below 0.1% and is one of the most accurate data sets currently available. Details of the experimental technique are given in the cited work and a review of the general principles is given in Ref. [16]. The statistical precision of the data was generally 0.02%. As shown in Fig. 1a, the full calculation of the XAS for Mo is in reasonable agreement with experiment over a broad spectral range. However, for both FEFF8.4 and FEFF9.0, the jump at the K-edge  $\mu_0$  and the amplitude of the XANES is smaller than that of the experimental data as seen in Fig. 1b. One source of this discrepancy appears to be the treatment of core-hole lifetime effects, which determines the shape of the threshold energy cutoff in the theory, and points to the need for improvements in the calculation of the background absorption cross-section  $\mu_0(E)$ . Another source of error near the edge is the neglect of the edge singularity effect of Mahan, Nozières, and De Dominicis (MND) [17–19]. Fig. 1c shows a comparison of calculations which include the MND effect (green) [20], calculations which do not include the effect (blue), and experiment (red). Qualitatively, the shape of the curve is improved when the MND effect is included, however, the

\* Corresponding author.

E-mail address: [jjr@uw.edu](mailto:jjr@uw.edu) (J.J. Rehr).

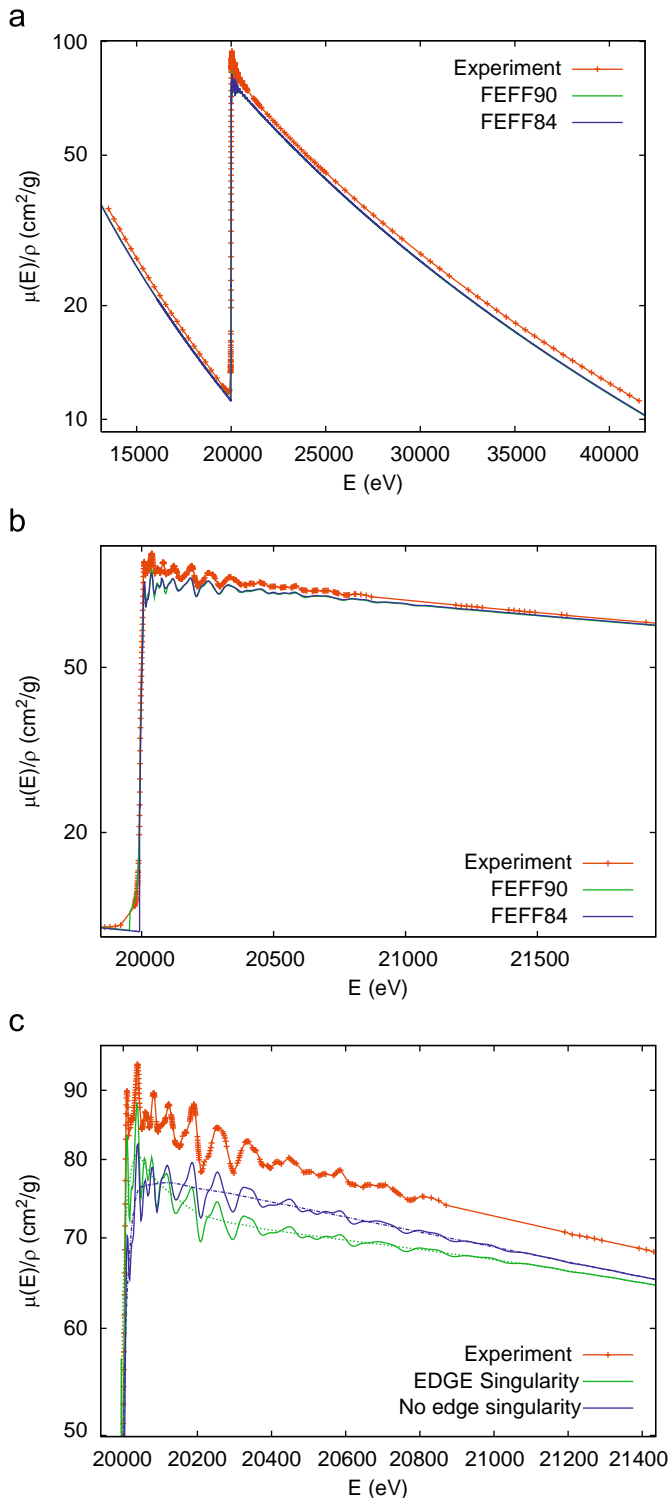


**Fig. 1.** Calculated mass absorption coefficient  $\mu(\omega)/\rho$  at the Mo K-edge compared to experiment. (a) Shows a comparison of experiment (red) to FEFF8.4 (blue) and FEFF9.0 (green). Note that the calculated results are low by  $\approx 3\text{--}4\%$  away from the edge, with the discrepancy becoming larger near the edge where the FMS and path expansion calculations are used. (b) Is the same as (a) except that the calculations have been multiplied by 1.03 in order to match the tails with experiment. Note that the disagreement is still large near the edge. Finally (c) shows calculations with (green) and without (blue) edge singularity effects compared to experiment (red). The atomic background calculations are shown as dashed lines. (For interpretation of the references to color in this figure legend, the reader is referred to the web version of this article.)

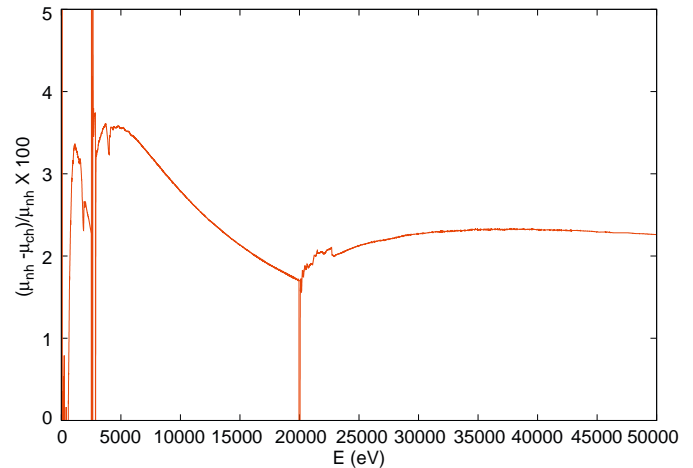


**Fig. 2.** Percent difference between calculations of  $\mu(\omega)/\rho$  at the Mo K-edge with and without a core-hole. Note that the calculation with a core-hole is smaller by 2–4% over the whole spectral range, not including small regions near the edges.

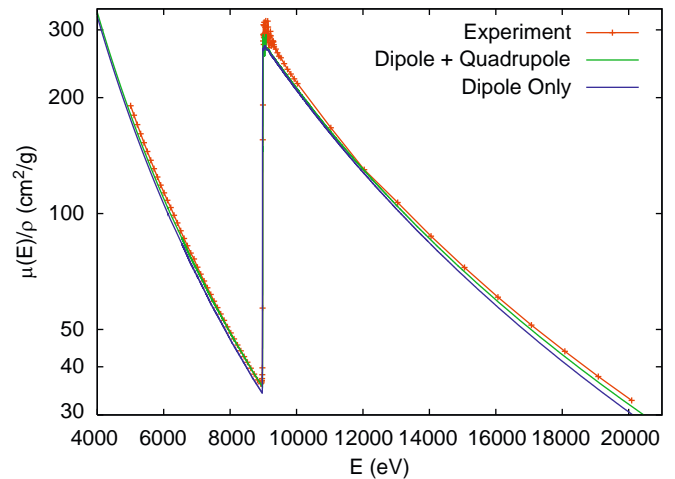


**Fig. 3.**  $\mu(\omega)$  at the Cu K-edge. Two calculations which neglect fine structure are compared to experiment (red) over a broad energy range. The first calculation includes quadrupole transitions (green), while the second does not (blue). (For interpretation of the references to color in this figure legend, the reader is referred to the web version of this article.)

reduction in weight starting at  $\approx 20\ 100\text{eV}$  is unexpected and may point to problems in our implementation of this effect. We have also investigated the effect of the core-hole on the calculation, and found that including a core-hole in our calculation reduces the absorption by 2–4% over the whole spectral range as shown in Fig. 2. This suggests a problem with the treatment of the many-body amplitude reduction factor  $S_0^2$ .

Fig. 3 shows a comparison of experiment (red pluses) to a calculation which includes quadrupole transitions (green), and one which includes only dipole transitions (blue) effects. Both calculations neglect fine structure. Clearly quadrupole transitions are important for an accurate description of the high energy tail of the spectrum.

Finally, in order to investigate solid state effects on the spectrum we compare a simulated atomic absorption calculation with the *embedded atomic background*  $\mu_0$  of bulk Cu, i.e. a calculation which includes solid state effects in the potential, but does not include fine structure. The FEFF code requires at least two atoms for any calculation; thus we simulated the Cu atomic absorption by calculating the absorption of a Cu–He diatomic

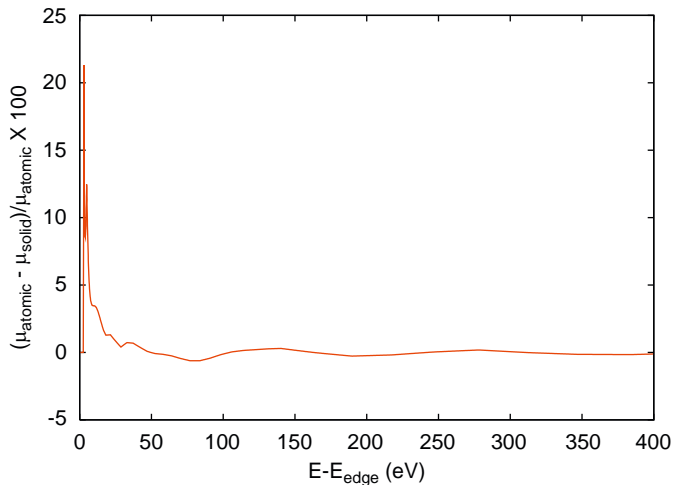


**Fig. 4.** Percent difference between an atomic calculation of  $\mu(E)$  (as described in the text) at the Cu K-edge and a calculation of the embedded atomic background  $\mu_0$  of bulk Cu.

molecule with a long bond length of 4 Å, for which the fine structure is very small compared to that in the solid. Fig. 4 shows the percentage difference between the calculated atomic absorption, and the embedded atomic background  $\mu_0$  of bulk Cu. Note that both calculations were performed with the FEFF9.0 code, which uses a muffin tin potential. Interestingly the only appreciable differences between the two calculations diminish rapidly with increasing energy, becoming negligible within a few tens of eV.

### 3. Comparison of XANES spectra

XANES calculations were performed using FEFF8.4 as well as FEFF9.0 to investigate the effects of several recently developed theoretical improvements available in FEFF9.0. These include the many-pole self-energy [8], the treatment of the core-hole within the random phase approximation (RPA) [6], and the many-body spectral function convolution [8]. The FEFF8.4 calculations by default include a fully screened core-hole using the final state rule (FSR). All of these calculations used self consistent potentials with a cluster radius of 6 Å, or equivalently, 58 atoms. The full multiple scattering (FMS) cluster size was 8 Å or 136 atoms. The correlated Debye model was used for all calculations with Debye temperatures of 380 K for Mo and 315 K for Cu, and temperatures of 294 K (Mo) and 10 K (Cu). Both the FEFF8.4 and FEFF9.0 calculations were shifted to align the white-line peak with experiment.

Figs. 5 and 6 show the results of several XANES calculations using different options in FEFF9.0. Fig. 5 compares the FEFF9.0 result including the RPA screened core-hole and many-pole self-energy, but neglecting the many-body spectral convolution to a calculation which includes the effect. The convolution with the many-body spectral function seems to be quite drastic at the edge, reducing the atomic background intensity too much. On the other hand, the fine structure amplitude is slightly improved for the first two peaks. The discrepancy at the edge could be due to the approximations that are made by performing an *a posteriori* convolution of the spectrum instead of convolving the Green's function.

Fig. 6 shows a comparison of experimental and theoretical K-edge XANES spectra of Cu. The FEFF9.0 calculation includes the RPA core hole treatment, the many-pole self-energy, and the spectral function convolution, while the FEFF8.4 calculation treats

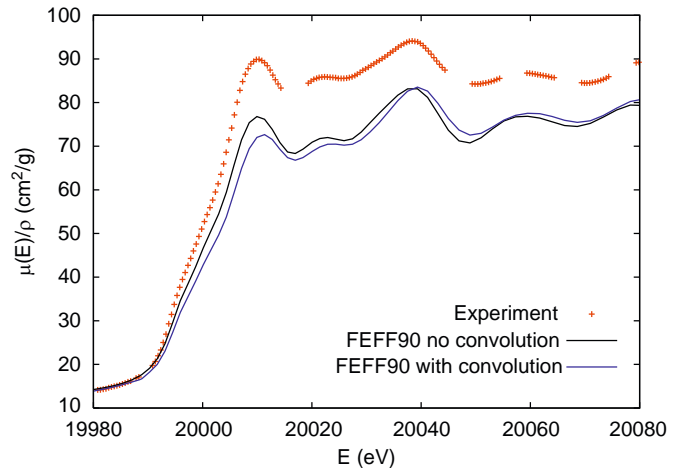


**Fig. 5.** Mo K-edge XANES spectra. Comparison of FEFF9.0 calculations with (blue) and without (black) the many body spectral function convolution. Experiment is also included (red). (For interpretation of the references to color in this figure legend, the reader is referred to the web version of this article.)

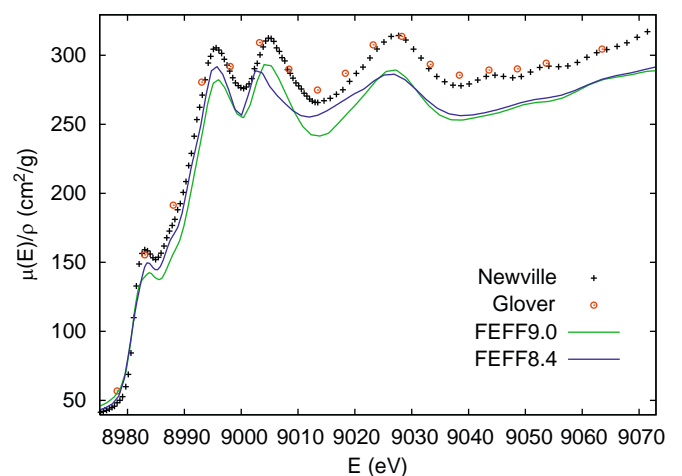


**Fig. 6.** Comparison of experimental (red circles) Cu K-edge XANES [21] with calculations from FEFF9.0 (green) and FEFF8.4 (blue). In order to compare the details of the XANES calculation with experiment we have also included additional experimental data (black+) [22,23], which has been scaled to match absolute measurement. (For interpretation of the references to color in this figure legend, the reader is referred to the web version of this article.)

the core hole via final state rule, and uses the Hedin–Lundqvist plasmon pole model self-energy. In this case, the agreement with experiment is clearly improved in both phases and amplitudes when FEFF9.0 is used instead of FEFF8.4.

### 4. Comparison of EXAFS fits

EXAFS comparisons can provide a sensitive test of theoretical models since the spectra depend crucially on various many-body effects and damping factors. Here we show K-edge EXAFS of Mo as calculated using both FEFF8.4 and FEFF9.0. The results were fit to the experimental data using the ARTEMIS and ATHENA fitting and preprocessing tools [14]. Fits were performed in *R*-space with a *k* range of 4.898–13.857 Å<sup>-1</sup>. Two different *R* ranges were used. The first included only the first shell with an *R* range of 1.700–3.523 Å, and the second included shells out to 5.5 Å.

Only four parameters were used in the fit: (1) an expansion parameter  $\beta$ , (2) a temperature parameter  $T = \alpha \times 300$  K

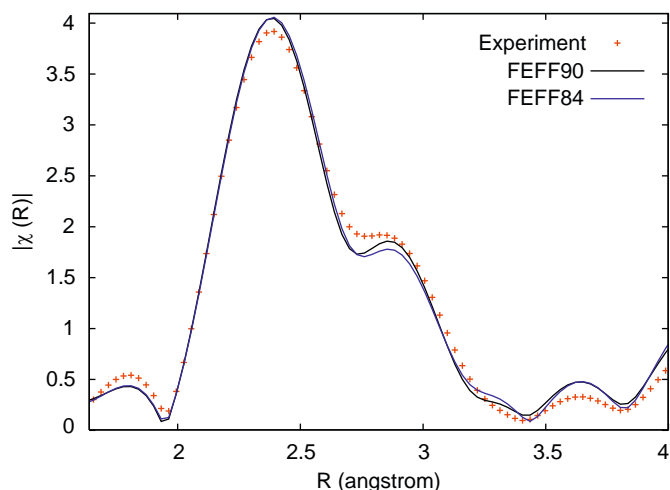


**Fig. 7.** Best first shell fits of FEFF8.4 (blue) and FEFF9.0 (black) compared to experimental (red) EXAFS signal in  $R$  space. The fit range was 1.700–3.523 Å. (For interpretation of the references to color in this figure legend, the reader is referred to the web version of this article.)

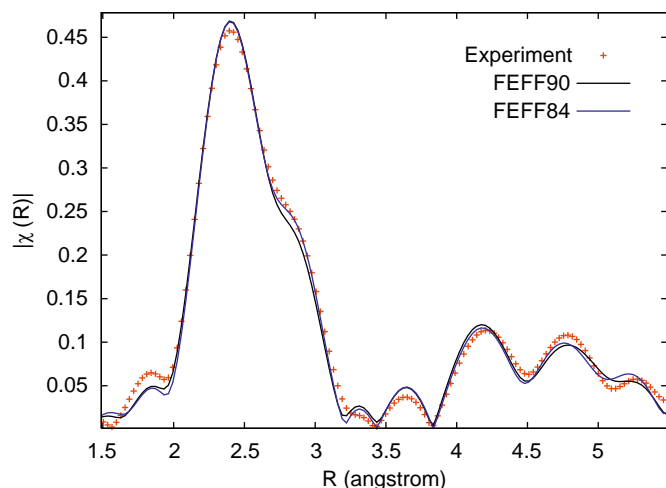


**Fig. 8.** Best large  $R$ -range fits of FEFF8.4 (blue) and FEFF9.0 (black) compared to experimental (red) EXAFS signal in  $R$  space. The fit range was 1.700–5.5 Å. (For interpretation of the references to color in this figure legend, the reader is referred to the web version of this article.)

which was used with a Debye temperature of 380 K to define the Debye–Waller factors, (3) an overall broadening factor  $E_i$ ; and (4) a shift of the edge  $\Delta E_0$ . The results of the first shell fit are shown in Fig. 7. For this fit, a slightly smaller  $\chi_{red}^2$  was obtained using FEFF8.4 than with FEFF9.0. The physical parameter values were consistent between FEFF8.4 and FEFF9.0.

There are discrepancies between the broadening factor  $E_i$  and the shift  $\Delta E_0$  in the two fits, but this is explained by the differences in the self-energy model. In particular,  $\Delta E_0$  is closer to zero for the fit to the FEFF9.0 calculation, indicating that the phase shifts between the XANES and EXAFS regions are in better agreement using the many-pole self energy than with the plasmon-pole self-energy. This is also supported by the comparison of the results of the XANES calculations with experiment. The difference in the results for the broadening factor  $E_i$  can also be explained by the fact that the temperature (Debye–Waller factor) is highly correlated with broadening.

The results of the large  $R$  range fits for both FEFF8.4 and FEFF9.0 are shown in Fig. 8. For this fit, a slight improvement in

**Table 1**

Fit statistics [ $N_p$  = number of independent points,  $N_v$  = number of variables,  $\chi^2$  and reduced- $\chi^2$ ,  $\Delta_k$  measurement uncertainty in  $k$ , and  $\Delta_R$  measurement uncertainty in  $R$ ]; final variable values, and final derived parameter values for large  $R$ -range fits [ $\sigma^2$  = Debye( $T$ , 380 K),  $r = R_{eff} \times \beta$ , and  $T = \alpha \times 300$  K].

Fitting statistic	FEFF8.4	FEFF9.0
$N_p$	22	22
$N_v$	4	4
$\chi^2$	557.2	419.5
$\chi_{red}^2$	31.84	23.97
$R$ -factor	0.01412	0.01063
$\Delta_k$	0.001	0.001
$\Delta_R$	0.003	0.003
<b>Variable</b>		
$\Delta E_0$	$3.3 \pm 0.8$	$1.50 \pm 0.6$
$E_i$	$0.3 \pm 0.5$	$1.4 \pm 0.4$
$\alpha$	$0.92 \pm 0.09$	$0.77 \pm 0.08$
$\beta$	$0.000 \pm 0.001$	$-0.002 \pm 0.001$
<b>Parameter</b>		
$\sigma^2$	0.0038	0.0032
$r$	2.73	2.72
$T$	280	230

$\chi_{red}^2$  was seen when using FEFF9.0. The parameters used in the fit were the same. Fitting statistics and final variable values are given in Table 1.

Although the statistics of these two fits are slightly different for FEFF8.4 and FEFF9.0, they appear to be consistent. The changes in reduced chi-squared are small compared to the deviation from the expected value, which points to the fact that there are still large systematic errors, possibly due to theoretical deficiencies.

## 5. Conclusion

Accurate data on an absolute scale raises serious challenges for theoretical computations. However, the complexity and detail of recent theoretical advances also enables insightful comparisons, and points to future directions in both theoretical and experimental developments. Broadening effects are clearly important, and understanding these better is crucial for further improvements. We compare recent developments along the extended XAFS range, and separately for the XANES region, with advanced experimental data sets for copper and molybdenum, which also invites further work.

## Acknowledgments

We thank M. Newville for comments. This work is supported in part by DOE Grant DE-FG03-97ER45623 (JJR, JJK) and NIH NCRR BTP Grant RR-01209 (JJK), and was facilitated by the DOE Computational Materials Science Network. We also acknowledge the ASRP and ARC for providing the funding for the experimental data used in this research.

## References

- [1] J.J. Rehr, R.C. Albers, Phys. Rev. B 41 (1990) 8139.
- [2] C.T. Chantler, J. Phys. Chem. Ref. Data 29 (2000) 597.
- [3] E. Cosgriff, C. Chantler, C. Witte, L. Smale, C. Tran, Phys. Lett. A 343 (2005) 174.
- [4] J.D. Bourke, C. Chantler, C. Witte, Phys. Lett. A 360 (2007) 702.

- [5] J.D. Bourke, C.T. Chantler, Finite difference method calculations of long-range X-ray absorption fine structure for copper over,  $k \approx 20 \text{ \AA}^{-1}$ , Nucl. Instr. and Meth. A, this special issue.
- [6] J.J. Rehr, J.J. Kas, M.P. Prange, A.P. Sorini, Y. Takimoto, F. Vila, C. R. Phys. 10 (2009) 548.
- [7] Y. Joly, Phys. Rev. B 63 (2001) 125120.
- [8] J. Kas, A.P. Sorini, M.P. Prange, L.W. Cambell, J.A. Soininen, J.J. Rehr, Phys. Rev. B 76 (2007) 195116.
- [9] C.T. Chantler, C.Q. Tran, D. Paterson, D. Cookson, Z. Barnea, Phys. Lett. A 286 (2001) 338.
- [10] C.T. Chantler, C.Q. Tran, Z. Barnea, D. Paterson, D. Cookson, D.X. Balaic, Phys. Rev. A 64 (2001) 062506.
- [11] C.Q. Tran, C.T. Chantler, Z. Barnea, Phys. Rev. Lett. 90 (2003) 257401.
- [12] C. Chantler, K. Olsen, R. Dragoset, J. Chang, A. Kishore, S. Kotochigova, D. Zucker, X-ray form factor, attenuation and scattering tables (version 2.1) [Online] (2005). URL: <http://physics.nist.gov/ffast>.
- [13] J.H. Hubbell, Natl. Stand. Ref. Data Ser. 69.
- [14] B. Ravel, M. Newville, J. Synchrotron Radiat. 12 (2005) 537.
- [15] M.D.D. Jonge, C.Q. Tran, C.T. Chantler, Z. Barnea, B.B. Dhal, D.J. Cookson, W.-K. Lee, A. Mashayekhiand, Phys. Rev. A 71 (2005) 032702.
- [16] C.T. Chantler, Eur. Phys. J. ST 169 (2009) 147.
- [17] G.D. Mahan, Phys. Rev. 163 (3) (1967) 612, doi: , doi:10.1103/PhysRev.163.612.
- [18] P. Nozières, D. Pines, Phys. Rev. 109 (3) (1958) 741, doi: , doi:10.1103/PhysRev.109.741.
- [19] P. Nozières, C.T. De Dominicis, Phys. Rev. 178 (3) (1969) 1097, doi:10.1103/PhysRev.178.1097.
- [20] L.W. Campbell, Inelastic losses in X-ray absorption theory, Ph.D. Thesis, University of Washington, 2002.
- [21] J.L. Glover, C.T. Chantler, Z. Barnea, N.A. Rae, C.Q. Tran, D.C. Creagh, D. Paterson, B.B. Dhal, Phys. Rev. A 78 (2008) 052902.
- [22] M. Newville, S.A. Carroll, P.A. O'Day, J. Synchrotron Radiat. 6 (1999) 276.
- [23] M. Newville, Ph.D. Thesis, University of Washington, 1995.